Study of Radical Merostabilization by Electrospray FTICR/MS

Alan R. Katritzky,*,§ Petia A. Shipkova,§ Ming Qi,§ Daniel A. Nichols,§ Richard D. Burton,§ Clifford H. Watson,§ John R. Eyler,*,§ Toomas Tamm,§ Mati Karelson,*,‡ and Michael C. Zerner*,§

Contribution from the Department of Chemistry, University of Florida, P.O. Box 117200, Gainesville, Florida 32611-7200, and the Department of Chemistry, University of Tartu, 2 Jakobi Str., Tartu, EE 2400, Estonia

Received June 17, 1996[⊗]

Abstract: The threshold fragmentation energies (E_o) of three different 4-(1′-substituted-2′-phenethyl)-1-methylpyridinium salts containing a neutral, an electron-donor, or an electron-acceptor group as α-substituent, respectively, were measured by Fourier Transform Ion Cyclotron Resonance Mass Spectrometry (FTICR/MS) collisionally activated dissociation (CAD). *N*-Methyl-4-(1-ethoxy-2-phenylethyl)pyridinium iodide (**10**), containing both electron-donor and electron-acceptor substituent groups, has a significantly lower E_o than the analogs containing a benzyl (**6**) or benzoyl (**7**) substituent. This was ascribed to merostabilization of the corresponding radical **19**, and this conclusion was further supported by theoretical calculations.

Introduction

It is well-known that electron-withdrawing substituents stabilize carbon anions and electron-donating substituents stabilize carbon cations. Dewar first suggested[1] that radicals should be particularly strongly stabilized when both an electron-attracting and an electron-donating substituent are present at the radical site. Katritzky[2a−d] provided the first experimental evidence for such carbon-containing radicals and proposed the term "merostabilization" to describe this concept. Balaban[3a−c] independently developed the analogous concept of "push-pull" for nitrogen centered radicals. Later, Viehe[4a−c] entered the field denoting these effects as "captodative". Merostabilization has been explained in terms of qualitative valence bond, molecular orbital and Linnett double quartet theories and supported by the prediction and synthesis of new stable radicals.[2b−d,3ac,4b] The concept provides a fundamental model for a better understanding of many properties of organic compounds, such as the chromophoric systems of indigo[5] and many heterocycles.[6]

However, further research on the stabilization of radicals by the synergistic interaction of substituents has given rise to much controversy. Whereas many research results supported the synergistic donor/acceptor stabilization[7,8] others suggested that the merostabilization concept was not universally valid. Thus, Rüchardt and co-workers provided evidence suggesting that stabilization effects are additive and not synergistic;[9a−d] Korth *et al.* indicated the absence of kinetic stabilization for some radicals by measuring their absolute rates for dimerization by ESR spectroscopy;[10] Chambers *et al.* revealed that the synergistic effect was not dominant in systems containing polyfluoroalkyl groups[11] and certain theoretical calculations failed to reveal any effect.[12]

Quantum mechanical calculations have been used to study merostabilization in radicals. Previous theoretical calculations from this group suggested that there was significant merostabilization energy in polar media, but not in the gas phase.[13a−c] Pasto[14] also found considerable extra stabilization in allyl-type three electrons radicals but not in other systems. Calculations had been carried out in water for carbon-centered radicals[15] and nitrogen-centered radicals,[16] all of which confirmed merostabilization in various situations. ESR spectroscopy was widely employed in those studies.[3c,17−19] Bordwell and co-workers determined radical stabilization energies by equilibrium acidities.[20] Most of this research was qualitative or semi-quantitative.

§ University of Florida.
‡ University of Tartu.
⊗ Abstract published in *Advance ACS Abstracts,* November 1, 1996.

(1) Dewar, M. J. S. *J. Am. Chem. Soc.* **1952**, *74*, 3353.
(2) (a) The early development of these ideas is contained in the MSc. Theses of R. W. Baldock (University of East Anglia, 1965) and of P. Hudson (University of East Anglia, 1971) (see also Ph.D. Thesis of P. Hudson, University of East Anglia, 1973). (b) Baldock, R. W.; Hudson, P.; Katritzky, A. R.; Soti, F. *Heterocycles* **1973**, *1*, 67. (c) Baldock, R. W.; Hudson, P.; Katritzky, A. R.; Soti, F. *J. Chem. Soc., Perkin Trans. I* **1974**, 1422. (d) Katritzky, A. R.; Soti, F. *J. Chem. Soc., Perkin Trans. I* **1974**, 1427.
(3) (a) Balaban, A. T. *Rev. Roum. Chim.* **1971**, *16*, 725. (b) Negoita, N.; Baican, R.; Balaban, A. T. *Tetrahedron* **1974**, *30*, 73. (c) Balaban, A. T.; Caproiu, M. T.; Negoita, N.; Baican, R. *Tetrahedron* **1977**, *33*, 2249.
(4) (a) Stella, L.; Janousek, Z.; Merényi, R.; Viehe, H. G. *Angew. Chem., Int. Ed. Engl.* **1978**, *17*, 691. (b) Viehe, H. G.; Merényi, R.; Stella, L.; Janousek, Z. *Angew. Chem., Int. Ed. Intl.* **1979**, *18*, 917. (c) Viehe, H. G.; Janousek, Z.; Merényi, R.; Stella, L. *Acc. Chem. Res.* **1985**, *18*, 148.
(5) Klessinger, M. *Angew. Chem., Int. Ed. Intl.* **1980**, *19*, 908.
(6) Katritzky, A. R.; Fan, W.-Q.; Li, Q.-L.; Bayyuk, S. *J. Heterocycl. Chem.* **1989**, *26*, 885.
(7) Humphreys, R. W. R.; Arnold, D. R. *Can. J. Chem.* **1979**, *57*, 2652.
(8) Crans, D.; Clark, T.; Schleyer, P. v. R. *Tetrahedron Lett.* **1980**, *21*, 3681.
(9) (a) Zamkanei, M.; Kaiser, J. H.; Birkhofer, H.; Beckhaus, H.-D.; Rüchardt, C. *Chem. Ber.* **1983**, *116*, 3216. (b) Birkhofer, H.; Hädrich, J.; Beckhous, H.-D.; Rüchardt, C. *Angew. Chem., Int. Ed. Engl.* **1987**, *26*, 573. (c) Beckhous, H.-D.; Rüchardt, C. *Angew. Chem., Int. Ed. Engl.* **1987**, *26*, 770. (d) Rakus, K.; Verevkin, S. P.; Keller, M.; Beckhaus, H.-D.; Rüchardt, C. *Liebigs Ann.* **1995**, 1483.
(10) Korth, H.-G.; Sustmann, R.; Merényi, R.; Viehe, H. G. *J. Chem. Soc., Perkin Trans. II* **1983**, 67.
(11) Chambers, R. D.; Grievson, B.; Kelly, N. M. *J. Chem. Soc., Perkin Trans. I* **1985**, 2209.
(12) Moyano, A.; Olivella, S. *J. Mol. Struct.* **1990**, *208*, 261.
(13) (a) Katritzky, A. R.; Zerner, M. C.; Karelson, M. M. *J. Am. Chem. Soc.* **1986**, *108*, 7213. (b) Karelson, M.; Tamm, T.; Katritzky, A. R.; Szafran, M.; Zerner, M. C. *Int. J. Quantum Chem.* **1990**, *37*, 1. (c) Karelson, M.; Katritzky, A. R.; Zerner, M. C. *J. Org. Chem.* **1991**, *56*, 134.
(14) Pasto, D. J. *J. Am. Chem. Soc.* **1988**, *110*, 8614.
(15) Takase, H. and Kikuchi, O. *J. Mol. Struct.* **1994**, *306*, 41.
(16) Kost, D.; Raban, M.; Aviram, K. *J. Chem. Soc., Chem. Commun.* **1986**, 346.
(17) Korth, H.-G.; Lommes, P.; Sustmann, R. *J. Am. Chem. Soc.* **1984**, *106*, 663.
(18) Maclnnes, I.; Walton, J. C. *J. Chem. Soc., Perkin Trans. II* **1987**, 1077.
(19) Himmelsbach, R. J.; Barone, A. D.; Kleyer, D. L.; Koch, T. H. *J. Org. Chem.* **1983**, *48*, 2989.
(20) Bordwell, F. G.; Zhang, X.-M. *Acc. Chem. Res.* **1993**, *26*, 510.

S0002-7863(96)02027-6 CCC: $12.00

We now report a quantitative evaluation of the merostabilization concept by Fourier Transform Ion Cyclotron Resonance Mass Spectrometry (FTICR/MS) in the gas phase.

We have previously measured appearance potentials[21a−e] from the threshold energies for fragment ion appearance in the collisionally activated dissociation (CAD) pathways of a variety of pyridinium cations. Most of this work utilized laser-desorption FTICR. Ultrahigh mass resolution, accurate and stable mass calibration, multiple stages of collisionally activated dissociation allowing tandem MS/MS, and extremely long ion storage times (>1 min) combine to make FTICR/MS a powerful method for studying organic cations in the gas phase. Most recently, we demonstrated that electrospray ionization coupled with FTICR/MS provides an excellent way to produce gaseous pyridinium ions from pyridinium salts in solution and to monitor the chemical behavior of the ions.[22] In studies of collisionally activated dissociation of pyridinium cations[21a,23,24] the *N*-methylpyridinium cation was found to be very stable, undergoing essentially no dissociation. Therefore, we selected a set of *N*-methylpyridinium salts as model compounds to investigate radical merostabilization.

Results and Discussion

Our general strategy was to investigate the way in which the energy for the homolytic scission of the 4-(*β*-phenethyl)-pyridinium cation would be affected by the presence of an electron donor or an electron acceptor substituent. If the merostabilization concept is correct, a suitably situated electron donor substituent should stabilize the pyridiniumylmethyl radical (Py^+-CH·-D) and hence facilitate the scission. The assumption here is that the C−C bond scission in all processes follows a similar potential energy curve, and that stabilization of the product determines the barrier; *i.e*. the intersection of the C−C bond breaking curve with the product formation curve. Thus, according to the Bell-Evans-Polanyi principle, the stabilization of the final state leads to the decrease of the transition barrier of the reaction.

Synthesis of Compounds. Three *N*-methylpyridinium salts were prepared (Scheme 1). 4-(Dibenzylmethyl)pyridine (**4**) and 4-(1,3-diphenyl-1-oxo-2-propyl)pyridine (**5**) were made starting from 4-picoline (**1**), by the sequential introduction either of two benzyl or of phenylacetyl and benzyl groups using modified literature methods.[25] These two substituted pyridines **4** and **5** reacted with methyl iodide to form the corresponding *N*-methylpyridinium salts **6** and **7**. Compound **10** was prepared from 1-pyridyl-2-phenylethanol (**9**) following the procedure indicated in Scheme 1.

Fragmentation Pathways. *N*-Methyl-4-(1,3-dibenzylmethyl)pyridinium iodide (**6**) (MW 415) was chosen as a model compound with a neutral substituent group. When CAD

Scheme 1. Synthesis of Compounds

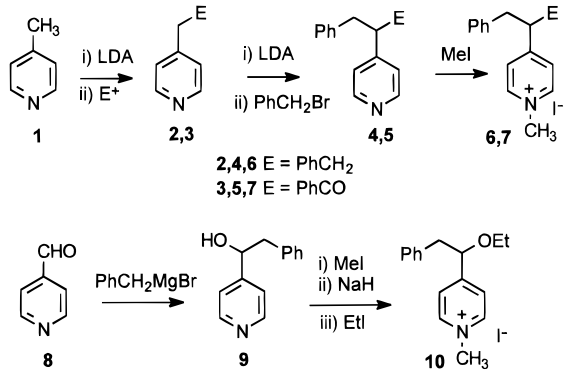

Scheme 2. Fragmentation Patterns of Compound **6**

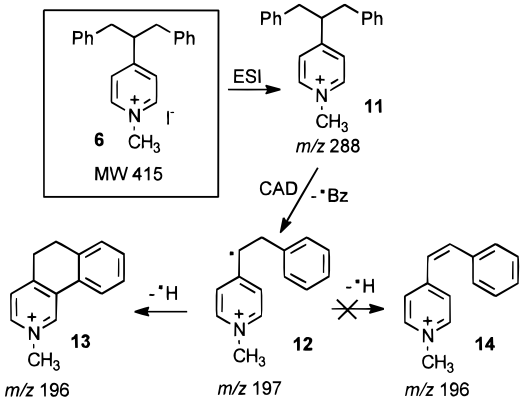

experiments were performed on the pyridinium cation **6**, the spectra showed three major ions (Scheme 2): (i) the parent cation **11** at *m/z* 288, (ii) the radical cation of interest **12** at *m/z* 197 generated *via* loss of a benzyl radical from the parent ion, and (iii) cation **13** at *m/z* 196, obtained *via* loss of a hydrogen atom from the radical **12**. The ion at *m/z* 196 may possess the cyclic structure **13**, formed *via* ring closure as shown on Scheme 2 rather than compound **14** with a double bond. Fragmentation leading to the formation of stable cyclic structures was previously observed by us in an independent study of singly and multiply charged pyridinium cations.[22] When the ion at *m/z* 197 was ejected, the ion at *m/z* 196 disappeared, proving that the ion at *m/z* 196 is formed from the radical at *m/z* 197 and not directly from the parent ion at *m/z* 288.

N-Methyl-4-(1,3-diphenyl-1-oxo-2-propyl)pyridinium iodide (**7**) (MW 429) was chosen as a model compound to study the effect of an electron withdrawing group (benzoyl) on the appearance potential. The CAD spectrum showed 5 major ions (Scheme 3): (i) the parent cation **15** at *m/z* 302, (ii) the radical cation **16** at *m/z* 211, corresponding to loss of a benzyl radical from the parent cation, (iii) cation **17** at *m/z* 210, generated *via* loss of a hydrogen atom from the radical **16**, (iv) the radical cation **12** at *m/z* 197 corresponding to loss of a benzoyl radical from the parent ion, and (v) the cation **13** at *m/z* 196, generated *via* loss of a hydrogen atom from the radical cation **12**. As in the case of compound **6** (Scheme 2) we believe that **13** is the right structural representation. When the ions at *m/z* 211 and *m/z* 197 were respectively ejected from the cell *via* standard double resonance experiments, the corresponding ions at *m/z* 210 and *m/z* 196 disappeared, confirming the proposed fragmentation sequence. Since two different radical fragmentations were observed, it could be expected that these species (**12** and **16**) would have similar appearance potentials, which was later confirmed experimentally and supported by theoretical calculations.

(21) (a) Katritzky, A. R.; Watson, C. H.; Dega-Szafran, Z.; Eyler, J. R. *J. Am. Chem. Soc.* **1990**, *112*, 2471. (b) Katritzky, A. R.; Watson, C. H.; Dega-Szafran, Z.; Eyler, J. R. *J. Am. Chem. Soc.* **1990**, *112*, 2479. (c) Katritzky, A. R.; Malhotra, N.; Dega-Szafran, Z.; Savage, G. P.; Eyler, J. R.; Watson, C. H. *Org. Mass Spectrom.* **1992**, *27*, 1317. (d) Katritzky, A. R.; Dega-Szafran, Z.; Watson, C. H.; Eyler, J. R. *J. Chem. Soc., Perkin Trans. II* **1990**, 1051. (e) Katritzky, A. R.; Dega-Szafran, Z.; Ramanathan, R.; Eyler, J. R. *Org. Mass Spectrom.* **1994**, *29*, 96.

(22) Katritzky, A. R.; Shipkova, P. A.; Burton, R. D.; Allin, S. M.; Watson, C. H.; Eyler, J. R. *J. Mass Spectrom.* **1995**, *30*, 1581.

(23) Watson, C. H.; Baykut, G.; Mowafy, Z.; Katritzky, A. R.; Eyler, J. R. *Anal. Instrum.* **1988**, *17*, 155.

(24) Katritzky, A. R.; Watson, C. H.; Dega-Szafran, Z.; Eyler, J. R. *Org. Mass Spectrom.* **1989**, *24*, 1017.

(25) Kaiser, E. M.; Petty, J. D. *Synthesis* **1975**, 705.

Scheme 3. Fragmentation Patterns of Compound **7**

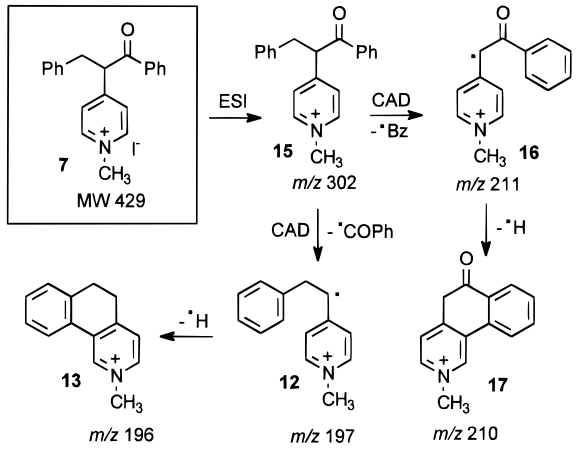

Scheme 4. Fragmentation Patterns of Compound **10**

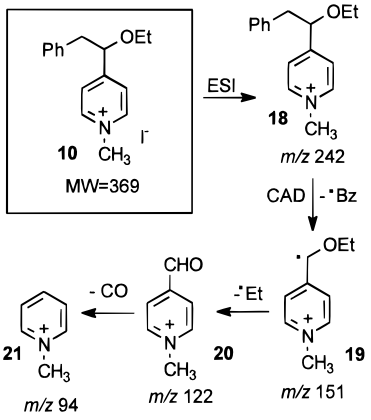

N-Methyl-4-(1-ethoxy-2-phenylethyl)pyridinium iodide (**10)** (MW 369) was chosen as a model compound to study the effect of an electron donating group (ethoxy) on the appearance potential of the corresponding radical. For the CAD experiments the precursor cation **18** (*m/z* 242) was isolated using standard RF ejection pulses and was allowed to undergo collisions with argon atoms. In addition to the parent ion **18**, the CAD spectrum showed formation of three fragment ions (Scheme 4): (i) *m/z* 151 generated *via* loss of a benzyl radical from the parent ion forming the radical cation of interest **19**; (ii) *m/z* 122 **20** corresponding to loss of ethyl radical from the radical cation **19**, and (iii) *m/z* 94 corresponding to methyl pyridinium ion **21**, generated *via* loss of a carbon monoxide molecule from the ion at *m/z* 122. To verify the fragmentation pathway we ejected the radical at *m/z* 151 and as a result, the ions **20** and **21** at *m/z* 122 and *m/z* 94 disappeared. It was thus confirmed that ions **20** and **21** are formed from fragmentation of the radical cation **19** and not directly from the parent ion.

Threshold Fragmentation Energies. Thresholds for the appearance of fragment ions allowed the estimation of threshold fragmentation energies (E_o) for the collisionally activated dissociation (CAD) in the gas phase of three substituted pyridinium cations to form the corresponding free radicals. The E_o values for the ions **11**, **15**, and **18** were calculated as previously described.[21a] The translational energy (E_{ion}) imparted to an ion during the excitation stage of the FTICR CAD process is obtained from eq 1,[26ab] where q is the ionic charge, V is the peak-to-peak amplitude of the RF excitation pulse, τ is the RF pulse width, m is the ionic mass, and d is the distance between the excitation plates of the analyzer cell.

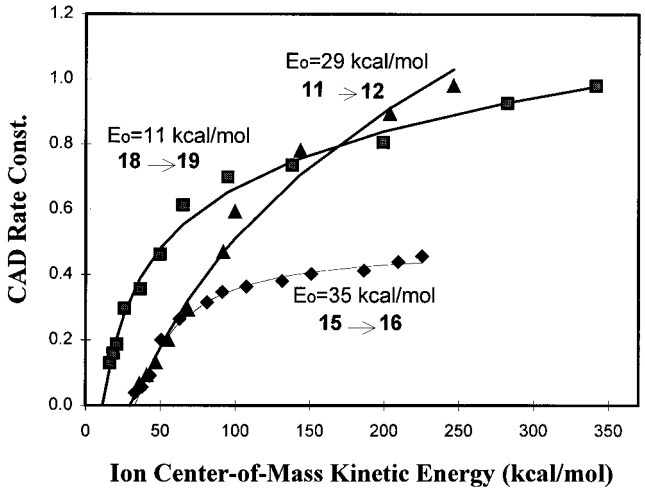

Figure 1. CAD rate constants plotted *vs*. ion center-of-mass kinetic energies (kcal/mol) to yield the threshold fragmentation energies E_o for cations **11**, **15**, and **18**. The symbols represent experimental measurements and the lines represent calculated fits from eqs 3 and 4.

$$E_{ion} = q^2V^2\tau^2/8md^2 \quad (1)$$

$$E_{cm} = E_{ion} \times [M_{Ar}/(M_{Ar} + m)] \quad (2)$$

The nominal center-of-mass energy (E_{cm}) can be calculated from eq 2, as described previously,[21a] where M_{Ar} is the mass of the neutral gas (Ar) and m is the mass of the ion. In our previous studies[21a−e] the nominal center-of-mass energy was plotted *vs* the percent fragmentation observed (I/I_o) and the straight line portions of these plots were extrapolated to zero fragmentation to give the observed threshold energy (E_{obs}). In the present study we used a program for analysis of CAD and ion/molecule reaction cross sections ("CRUNCH"), written by Armentrout and Ervin.[27] We have modified slightly the fitting function in that program to be more appropriate to the FTICR CAD conditions as shown in eq 3, where k is the observed CAD rate constant, k_o is an energy-independent scaling factor, E_o is the threshold energy and v is treated as a variable parameter. This functional form has been predicted for CAD processes and Armentrout *et al.* have shown experimental proof that it provides accurate CAD thresholds.[28]

$$k = k_o(E - E_o)^v/E \quad (3)$$

$$ln(I_o/I) = knt \quad (4)$$

The CAD rate constants are derived from the percent fragmentation observed (eq 4), where (I/I_o) is the percent fragmentation observed, n is the number density of the collision gas and t is the CAD reaction time. Plots of CAD rate constants *vs* center-of-mass kinetic energy for all three cations **11**, **15**, and **18** are shown in Figure 1. In a previous study[21a] absolute experimental errors in calculating E_o values were estimated to be up to 0.35 eV (8 kcal/mol), and relative experimental errors are expected to be lower for comparable systems. The experimental errors in the present report are expected to fall in the same range.

Radical Merostabilization. As seen in Figure 1, and determined from the computer fits (CRUNCH program) the

(26) (a) Cody, R. B.; Burnier, R. C.; Freiser, B. S. *Anal. Chem.* **1982**, *54*, 96. (b) Bensimon, M.; Houriet, R. *Int. J. Mass Spectrom. Ion Processes* **1986**, *72*, 93.

(27) Ervin, K. M., Armentrout, P. B. *J. Chem Phys.* **1985**, *83*, 166.
(28) Aristov, N.; Armentrout, P. B. *J. Phys. Chem.* **1986**, *90*, 5135.

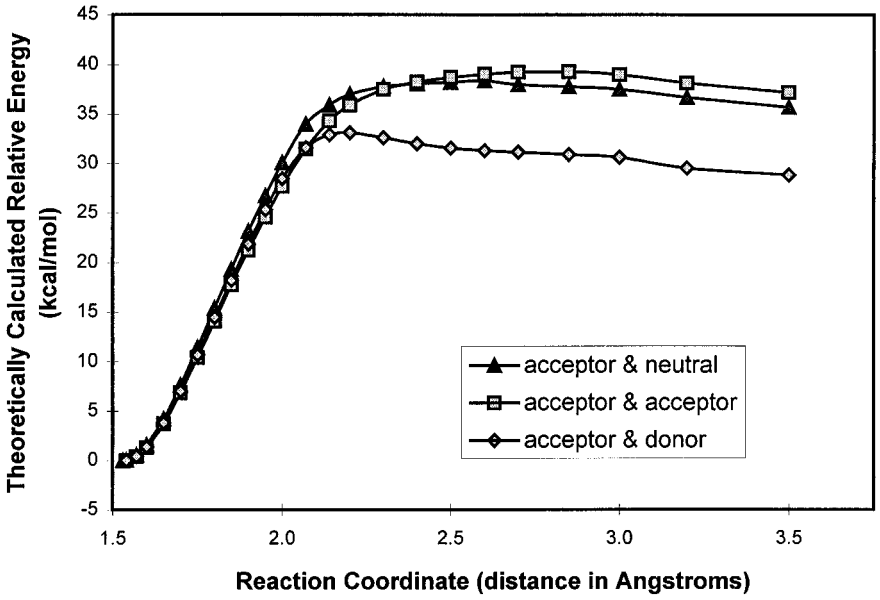

Figure 2. Theoretically calculated relative energy (kcal/mol) plotted *vs*. reaction coordinate. The reaction coordinate listed is the distance of the C−C bond being broken, minimizing the energy with respect to all other molecular coordinates.

observed threshold fragmentation energies (E_o) for pyridinium cations **11**, **15**, and **18** are 29 kcal/mol, 35 kcal/mol and 11 kcal/mol, respectively. Assuming no significant difference in ground state stabilization of the starting materials, a lower E_o means higher stability of the corresponding radical. Therefore, radical **19** demonstrated significant stabilization ($\Delta E_o \approx 20$ kcal/mol) compared to radical **12**, (which has only one electron-accepting group: pyridinium ion Py+) and radical **16**, (which has two electron-accepting groups: pyridinium ion and benzoyl). This strongly supports the concept of radical merostabilization, that an electron-accepting group (pyridinium ion) and an electron-donating group (ethoxy) can significantly stabilize a radical. The pyridinium ion is a very effective electron-accepting group and only a very small difference of stabilization was found between radicals **12** and **16**, and as expected pyridinium cation **15** gave two radicals, **12** and **16,** in the CAD experiments.

Theoretical Calculations. To support the experimental results, AM1[29] and PM3[30] quantum-chemical calculations were performed, using the Unrestricted Hartree−Fock (UHF) Hamiltonian as implemented in the AMPAC 5.0 program package.[31] Neither of these semiempirical methods has been parametrized specifically for calculation of the properties of transition states involving radical species or UHF wavefunctions. It was therefore considered necessary to perform these calculations with both parameterizations (AM1 and PM3) in parallel to decrease the chances of model errors biasing the results. As shown later, the results obtained are similar for the two parametrizations used. In general the AM1 model produces heats of formation within ±7 kcal/mol and the PM3 model ±4 kcal/mol for compounds of this type.[32] Neutral closed-shell systems are more accurately reproduced than are radicals and cations.[32] Since we are comparing energy differences for rather similar processes we expect that such errors are systematic. Considerably less is known about barriers to reactions, and the UHF method, in general, might be expected to overestimate them. Comparison of the observed fragmentation energies with our calculated barriers suggest that this might be the case in the present study: the energy required to break a C−C single bond could be somewhat too high. The relative barriers, however, depend on the intersection of this potential energy surface with that of the relative heats of formation of the products. Throughout all the calculations, all stationary points were additionally characterized by calculations of the Hessian (force-constant) matrix. All minima were confirmed with no negative eigenvalues and all transition state geometries had a single negative eigenvalue of the Hessian.

Due to the nature of the semiempirical parametrization, the zero-point vibrational energies are included in the parameters and need not be added explicitly. This assumption was verified for several calculated geometries and energy differences. It was, indeed, found that the inclusion of the zero-point energies did not affect the results significantly.

Dissociation paths were initially characterized by stepwise increasing the length of the breaking bond, while optimizing all other coordinates at each given bond length. The resulting potential energy curves are presented in Figure 2. From the points with the highest energy, the transition state geometries were refined using the eigenvector following procedure.[33] It can be concluded that the height of the reaction barrier ($\Delta H^{\ddagger}$), as well as the overall thermodynamic stabilization are about 10 kcal/mol lower for cation **18** (see Table 1), containing an electron-donor and an electron-acceptor group as compared to cations with one neutral and one electron-accepting group (**11**) or two electron-accepting groups (**15**) attached in the dissociation product to the carbon radical center.

In another series of calculations, full geometry optimizations were performed for the reactants and products of the dissociation reactions, as well as for a series of similar comparison reactions, where the electron-accepting methylpyridinium group was replaced by a neutral phenyl group; in these compounds (**22**, **23**, and **24**) (see Scheme 5) with the effect of an electron-

(29) Dewar, M. J. S.; Zoebisch, E. G.; Healy, E. F.; Stewart, J. J. P. *J. Am. Chem. Soc.* **1985**, *107*, 3902.
(30) Stewart, J. J. P. *J. Comput. Chem.* **1989**, *10*, 209.
(31) AMPAC 5.0; Semichem, Inc.: 7128 Summit, Shawnee, KS 66216, 1994.
(32) Zerner, M. C. In *Reviews of Computational Chemistry*; Lipkowitz, K. B., Ed.; VCH: New York, 1991; Vol. 2.
(33) Baker, J. *J. Comput. Chem.* **1986**, *7*, 385.

Table 1. Theoretically Calculated Heats of Reaction (ΔH_R) and Energies of Transition States ($\Delta H^{\ddagger}$) (all in kcal/mol)

	compounds and groups[a]								
	11 A and N		**15** A and A		**18** A and D		**22** N and N	**23** N and A	**24** N and D
	$\Delta H^{\ddagger}$	ΔH_R	$\Delta H^{\ddagger}$	ΔH_R	$\Delta H^{\ddagger}$	ΔH_R	ΔH_R	ΔH_R	ΔH_R
AM1	38	38	39	40	31	32	33	35	33
PM3	37	36	41	41	32	29	33	36	32

[a] D = electron donor; A = electron acceptor; N = neutral.

Scheme 5. Structures for Compounds **22**, **23**, and **24**

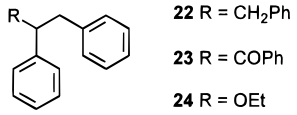

Scheme 6. Structures **25**−**32** for Calculation of Merostabilization Energies

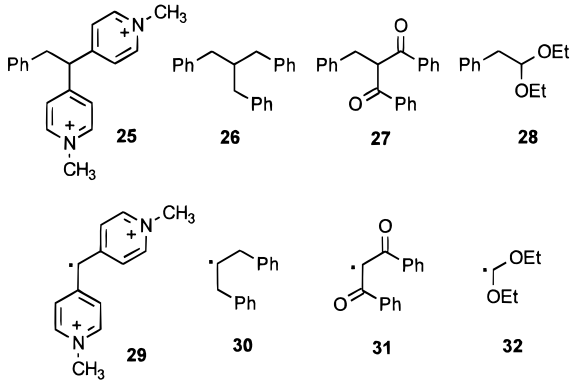

acceptor substituent eliminated, no radical stabilization should be found. Heats of radical formation (ΔH_R) were calculated for all cases as summarized in Table 1. The dissociation energy of cation **18** is significantly lower than that of the cations **11** or **15**, in agreement with the experimental results. However, where the electron-accepting group (pyridinium) is replaced by a neutral group (phenyl) no evidence for stabilization is found not only in the heats of the dissociation reaction of compounds **22** and **23** but also in that for **24**. For compounds **15** and **18**, the AM1 calculated transition state energies ($\Delta H^{\ddagger}$) are slightly lower than the corresponding heats of radical formation (ΔH_R), due to the different methods of calculation of these quantities. The ΔH_R calculations involved heats of formation of isolated products (corresponding to infinite separation), whereas in the $\Delta H^{\ddagger}$ calculations, the products were separated by a small finite distance and the energy of the system is lowered by the charge-dipole interactions between the products.

The merostabilization energy (E_M) of a radical with an electron-donor (D) and an electron-acceptor (A) groups attached simultaneously to the carbon radical center (*e.g.* radical **19**) is defined as shown in eq 5, where E_{DA} is the energy of the radical studied (**19**), E_{DD} is the energy of a radical with two electron-donor groups (such as radical **32**, Scheme 6) and E_{AA} is the energy of the radical with two electron-acceptor groups at the radical center (such as radical **29**, Scheme 6).

The calculated merostabilization energy (E_M) of radical **19** is artificially lowered because the heat of formation of the AA species (E_{AA}) is additionally enhanced due to the intramolecular charge-charge repulsion between two positively charged methyl pyridinium groups. In order to eliminate this contribution to the merostabilization energy, we have used the difference between the calculated E_M values of the parent ion **18** ($E_{M\,ion}$, calculated using structures **18**, **28**, and **25**, respectively) and of the radical **19** ($E_{M\,rad}$) as the characteristics of the merostabilization (eq 6).

$$E_M = E_{DA} - {}^1/_2(E_{DD} + E_{AA}) \tag{5}$$

$$\Delta E_M = (E_{M\,rad}) - (E_{M\,ion}) \tag{6}$$

When both an electron-donor (OEt) and an electron-acceptor (methylpyridinium) group are present, as for radical **19**, a significant additional stabilization of the radical was observed ($\Delta E_M \sim 8-10$ kcal/mol) (see Table 2). For a comparison, the calculated analogous energy difference (ΔE_M) was much smaller for radicals **12** and **16**, containing the electron-accepting methylpyridinium group and the mesomerically inactive benzyl group, and two electron-acceptor groups (benzoyl and methylpyridinium), respectively (see Table 2). [For ion **11**, E_{DD} is calculated from **26** and E_{AA} from **25**. For ion **15**, E_{DD} is calculated from **27** and E_{AA} from **25**. For ion **18**, E_{DD} is calculated from **28** and E_{AA} from **25**. For radical **12**, E_{DD} is calculated from **30** and E_{AA} from **29**. For radical **16**, E_{DD} is calculated from **31** and E_{AA} from **29**. For radical **19**, E_{DD} is calculated from **32** and E_{AA} from **29**.] Therefore, our calculations indicate the presence of a certain merostabilization of the radical with an electron-accepting and an electron-donating group simultaneously bonded to a carbon radical center.

Conclusion

The existence of merostabilization in the system investigated is supported by both our experimental and theoretical calculations. It was clearly shown that when both an electron-donor and an electron-acceptor group are present at the radical site, significant additional stabilization was achieved. For comparison, when in the same system the electron-donor group was replaced by an electron-acceptor or a neutral group, no additional stabilization was observed.

Experimental Section

ESI Source. A modified dual-stage hexapole ion-guide ESI source (Analytica of Branford, Branford, CN) was used for this work. The normal glass capillary (0.5 mm I.D. × 150 mm) used with nitrogen counter-current drying gas was replaced by a heated metal capillary of similar dimensions. The metal capillary was mounted in a brass support and heated with a 200 W cartridge heater. The temperature was maintained at 120 °C using an RTD (Resistive Thermal Device) temperature controller which regulated the heater power supply. The source was operated without a counter-current drying gas.

Ions were sprayed from a needle maintained at a potential of +3.9 kV. The pressure between the capillary exit and the first skimmer (1.0 mm diameter) was maintained at 1 mbar with a 500 L/min mechanical pump (Edwards, Model EM32). The pressure between the first skimmer and conductance limit (1 mm diameter) located in the center of the hexapole ion-guide was maintained at *ca.* 1×10^{-3} mbar with a turbo drag pump (Edwards, Model EXT250HI) as measured using a Pirani gauge (TPR 010, Balzers AG, Liechtenstein). The pressure after the ESI hexapole guide in the normal FTICR external source housing was *ca.* 1.0×10^{-6} mbar as pumped by an 800 L/s cryopump.

Table 2. Calculation of Merostabilization Energies[a]

	heat of formation			$E_{M\,ion}$	heat of formation			$E_{M\,rad}$	ΔE_M
I: Neutral and Acceptor Substituents									
cpds	**11**	**25**	**26**	**11**	**12**	**29**	**30**	**12**	
AM1	217	441	53	−30	216	441	56	−32	−2
PM3	217	436	54	−28	213	432	59	−32	−4
II: Acceptor and Acceptor Substituents									
cpds	**15**	**25**	**27**	**15**	**16**	**29**	**31**	**16**	
AM1	197	441	9	−28	198	441	15	−30	−2
PM3	191	436	4	−29	192	432	9	−29	0
III: Donor and Acceptor Substituents									
cpds	**18**	**25**	**28**	**18**	**19**	**29**	**32**	**19**	
AM1	152	441	−90	−24	145	441	−83	−34	−10
PM3	154	436	−76	−25	144	432	−78	−33	−8

[a]All values are given in kcal/mol.

The samples were dissolved in 49/49/2 (volume ratio) water/methanol/acetic acid solution at a concentration of 0.1 mg/mL and were introduced into the ESI source at a flow rate of 1 μL/min.

External Source FTICR. All experiments were carried out using a Bruker BioAPEX 7e external source FTICR spectrometer (Bruker Analytical Systems, Inc., Billerica, MA) equipped with a horizontal bore, room-temperature, 15 cm inside diameter, 7 T superconducting magnet, an external source, and a 170 mm^3 cylindrical RF-shimmed Infinity analyzer cell.[34] The standard external source FTICR instrument has been previously described.[35] Problems associated with installation of the nominal 7 tesla magnet resulted in using the magnet, during this study, energized only to 4.7 tesla. The FTICR external source design has two stages of differential pumping which produce a pressure differential of up to 10^5 between the external source and analyzer regions. The high and ultrahigh vacuum regions were maintained using cryopumps (Edwards High Vacuum Co., Woburn, MA). An 800 L/s cryopump (N_2) was used to pump the high gas load region of the external source vacuum compartment where ions exiting the ESI source were accelerated toward the mass analyzer using a series of electrostatic optics. A 400 L/s cryopump evacuated the region between the first and second conductance limits that contained the electrostatic ion transfer optics. An additional 400 L/s cryopump was used to maintain the ultrahigh vacuum in the analyzer region.

After exiting the high pressure ESI source and entering the electrostatic ion optics, ions were accelerated to 2.5 kV and tightly focused through the two conductance limits before being accumulated and trapped in the FTICR analyzer cell.[35] Since the ions were continuously produced by the ESI source a set of x-, y-deflection plates were gated "open" during the ion accumulation period for 50 to 200 ms to allow time for ions to accumulate. The trapped ions were resonantly excited using a swept frequency RF "chirp". Ions were detected using the broadband detection mode covering a mass range from 50 to 5000 amu. Typically, 25 individual transients were co-added to improve the signal-to-noise ratio. The raw time-domain transients were apodized[36] and zero-filled[37,38] three times prior to Fourier transformation.

The experimental event sequence for obtaining ESI/FTICR mass spectra began with a 50 ms quench pulse to remove any ions remaining in the cell from a previous measurement cycle. After the quench pulse, an ion accumulation event followed, which allowed accumulation of ions in the analyzer cell. Precursor ions were isolated using swept-frequency ejection pulses of *ca*. 100 to 400 ms duration to eject all other ions. A pulsed valve introduced the argon collision gas prior to ion activation. With the pulsed valve open for 50 μs a peak pressure of 3×10^{-7} mbar was obtained. The precursor ions were excited using a variable amplitude on-resonance excitation pulse of 10 μs duration. A 50 to 250 volt range of RF amplitudes was used to study the energy dependence of the collisionally activated dissociation process. The amplitude of the RF excitation was measured directly on the cell plates using a calibrated oscilloscope and the obtained values were used for the calculations (eq 1). A delay of 0.5 s following the precursor ion's excitation allowed time for the translationally excited precursor ion to undergo collisions and fragment prior to the excitation/detection events. A schematic diagram of the pulse sequence is shown in Figure 3.

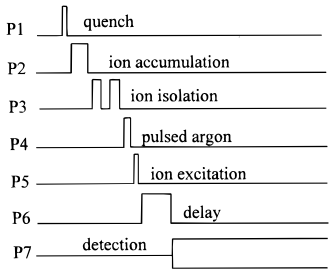

Figure 3. Pulse sequence for CAD experiments.

General Procedure for Synthesis of Compounds 2−5. To a stirred THF solution of starting material, LDA (1.5 M solution in cyclohexane, 1.1 equiv) was added dropwise at −78 °C under nitrogen atmosphere, the resulting mixture was allowed to stir for 1 h. Then, a solution of appropriate electrophile (1 equiv) in THF was added slowly. The reaction mixture was stirred for a further 2 h at −78 °C and then allowed to warm to room temperature. After general workup, the crude product was purified by column chromatography to give the pure compound. For 4-dibenzylmethylpyridine (**4**), a mixture of 4-phenylethylpyridines **2** and **4** (70:30) was obtained and could not be separated by column chromatography. The pure compound **4** was obtained by preparative GC.

4-Phenylethylpyridine (2): white microcrystals, 90% yield, mp 69−71 °C [lit.[39] 70−70.8 °C] (Found C, 85.04; H, 7.35; N, 7.59. $C_{13}H_{13}N$ requires C, 85.21; H, 7.15; N, 7.64%); ^{1}H NMR δ 2.89 (4H, s), 7.05 (2H, d, J = 6.7 Hz), 7.12−7.32 (5H, m) and 8.46 (2H, d, J = 6.7 Hz); ^{13}C NMR δ 36.5, 37.0, 121.0, 123.9, 126.2, 128.3, 128.4, 140.6, 149.7 and 150.4; MS *m/z* 183 (M^+, 44%), 91 (100).

4-(Phenylacylmethyl)pyridine (3): white microcrystals, 25% yield, mp 112−114 °C [lit.[40] 113−115 °C] (Found C, 79.40; H, 5.72; N, 7.19. $C_{13}H_{11}NO$ requires C, 79.19; H, 5.62; N, 7.10%); ^{1}H NMR δ 4.31 (2H, s), 7.22 (2H, d, J = 5.8 Hz), 7.48−7.53 (2H, m), 7.59−7.64 (1H, m), 8.0−8.03 (2H, m) and 8.58 (2H, d, J = 5.6 Hz); ^{13}C NMR δ 44.5, 124.8, 128.7, 128.8, 133.5, 136.1, 143.4, 149.9 and 195.8; MS *m/z* 197 (M^+, 10%), 105 (100).

4-Dibenzylmethylpyridine (4): white microcrystals, mp 70−72 °C [lit.[39] 71.5−73 °C] (Found C, 87.56; H, 7.20; N, 5.10. $C_{20}H_{19}N$ requires C, 87.87; H, 7.01; N, 5.12%); ^{1}H NMR δ 2.89 (2H, dd, J = 8.5, 13.5 Hz), 3.02 (2H, dd, J = 6.2, 13.5 Hz), 3.10−3.20 (1H, m), 6.93−7.01 (6H, m), 7.14−7.26 (6H, m) and 8.40 (2H, d, J = 6.1 Hz); ^{13}C NMR δ 41.8, 49.5, 123.4, 126.2, 128.3, 129.0, 139.4, 149.6 and 153.1; MS *m/z* 273 (M^+, 67%), 182 (75), 91 (100).

4-(1,3-Diphenyl-1-oxo-2-propyl)pyridine (5): white microcrystals, 35% yield, mp 108−110 °C (Found C, 84.03; H, 6.09; N, 4.78. $C_{20}H_{17}$-

(34) Caravatti P.; Allemann, M. *Org. Mass Specrom.* **1991**, *26*, 514.
(35) Kruppa, G. H.; Caravatti, P.; Radloff, C.; Zürcher, S.; Laukien, F.; Watson, C; Wronka, J. In *FT-ICR/MS: Analytical Applications of Fourier Transform Ion Cyclotron Resonance Mass Spectrometry*; Asamoto, B., Ed.; VCH: New York, 1991; Chapter 4, pp 107.
(36) Lee, J. P.; Comisarow, M. B. *Appl. Spectrom.* **1989**, *43*, 599.
(37) Bartholdi, E.; Ernst, R. R. *J. Magn. Resonance* **1973**, *11*, 9.
(38) Comisarow, M. B.; Melka, J. D. *Anal. Chem.* **1979**, *51*, 2198.
(39) Avramoff, M.; Sprinzak, Y. *J. Am. Chem. Soc.* **1956**, *78*, 4090.

NO requires C, 83.60; H, 5.96; N, 4.87%); ^{1}H NMR δ 3.07 (1H, dd, J = 7.7, 13.8 Hz), 3.55 (1H, dd, J = 7.1, 13.7 Hz), 4.81 (1H, t, J = 7.2 Hz), 7.05−7.07 (2H, m), 7.16−7.27 (5H, m), 7.36−7.41 (2H, m), 7.48−7.50 (1H, m), 7.86−7.89 (2H, m) and 8.50 (2H, br s); ^{13}C NMR δ 39.7, 55.1, 123.4, 123.5, 126.5, 128.4, 128.6, 128.7, 129.0, 133.3, 138.7, 147.8, 150.2 and 198.1; MS *m/z* 287 (M^+, 18%), 105 (100).

General Procedure for Synthesis of *N*-Methylpyridinium Salts 6 and 7. The appropriate substituted pyridine **4** and **5** was reacted with excess methyl iodide in methylene chloride at room temperature. The reaction was monitored by ^{1}H NMR. After the reaction was complete, the reaction mixture was concentrated, and the residue was purified by recrystalization to give the pure pyridinium salt.

***N*-Methyl-4-(1,3-diphenyl-2-propyl)pyridinium iodide (6)**: white microcrystals, 90% yield, ^{1}H NMR δ 2.96 (2H, dd, J = 8.9, 13.9 Hz), 3.15 (2H, dd, J = 6.2, 14.0 Hz), 3.49−3.53 (1H, m), 4.58 (3H, s), 7.03 (4H, d, J = 6.9 Hz), 7.13−7.29 (6H, m), 7.68 (2H, d, J = 6.6 Hz), and 9.10 (2H, d, J = 6.5 Hz); ^{13}C NMR δ 41.0, 48.6, 50.1, 126.9, 127.5, 128.8, 128.9, 137.4, 144.6 and 164.8.

***N*-Methyl-4-(1,3-diphenyl-1-oxo-2-propyl)pyridinium Iodide (7).** In this case, the residue was very difficult to purify by recrystallization, but it was verified that the major part of the residue was **7** by NMR and FTICR/MS. ^{1}H NMR δ 3.19 (1H, dd, J = 7.5, 13.6 Hz), 3.56 (1H, dd, J = 7.3, 13.4 Hz), 4.55 (3H, s), 5.36 (1H, t, J = 7.4 Hz), 7.10−7.30 (7H, m), 7.40−7.65 (3H, m), 8.05−8.10 (2H, m) and 9.02 (2H, d, J = 6.7 Hz); ^{13}C NMR δ 40.2, 49.1, 54.3, 127.4, 128.4, 128.9, 129.0, 129.2, 130.1, 130.6, 133.5, 134.4, 136.3, 142.3, 144.9, 158.6 and 196.5.

1-Pyridyl-2-phenylethanol (9). Benzylmagnesium bromide (1.2 equiv, 1.0 M ether solution) was added slowly to a cooled (−78 °C) solution of 4-pyridinylcarboxaldehyde in dry THF. The reaction mixture was allowed to warm to room temperature overnight. After usual aqueous workup, the product was obtained by flash column chromatography as a solid, yield 40%, mp 145−147 °C [lit.[41] 146−147.5 °C]; ^{1}H NMR δ 2.90−3.05 (2H, m), 3.35 (1H, br s), 4.85−4.90 (1H, m), 7.10−7.30 (7H, m) and 8.42 (2H, d, J = 6.0 Hz); ^{13}C NMR δ 45.7, 73.7, 120.9, 126.9, 128.6, 129.5, 137.0, 149.6 and 152.9; MS *m/z* 199 (M^+, 4%), 108 (72) and 92 (100).

***N*-Methyl-4(1-benzyl-1-ethoxy)methylpyridinium Iodide (10).** Compound **9** was first reacted with excess iodomethane in methylene chloride at rt to form *N*-methyl pyridinium salt. The excess MeI and solvent was removed under vacuum. The residue was dissolved in dry THF under nitrogen atmosphere, sodium hydride was added at 0 °C, then warm to rt. Then, ethyl iodide (2 equiv) was added and heated to reflux for 10 h. The reaction mixture was concentrated, dissolved in CH_2Cl_2, washed by H_2O, and dried. The solvent was removed to give a mixture, which was difficult to purify, but shown to contain **10** as the major component by NMR and FTICR/MS. ^{1}H NMR δ 1.16 (3H, t, J = 7.0 Hz), 3.40 (1H, dd, J = 5.8, 13.8 Hz), 3.43 (1H, dd, J = 6.8, 13.8 Hz), 3.61 (2H, q, J = 7.0 Hz), 4.64 (3H, s), 4.73−4.77 (1H, m), 7.10 (2H, d, J = 7.8 Hz), 7.21−7.29 (3H, m), 7.84 (2H, d, J = 6.4 Hz) and 9.15 (2H, d, J = 6.5 Hz); ^{13}C NMR δ 15.1, 43.2, 49.0, 66.1, 80.7, 125.5, 127.0, 128.4, 129.2, 129.6, 135.4, 144.9 and 162.7.

JA962027H

(40) Smith, Jr. J. M.; Stewart, H. W.; Roth, B.; Northey, E. H. *J. Am. Chem. Soc.* **1948**, *70*, 3997.

(41) Traynelis, V. J.; Yamauchi, K.; Kimball, J. P. *J. Am. Chem. Soc.* **1974**, *96*, 7289.